The University of Queensland
Australia

Global Change Institute

June 2016

DISCUSSION PAPER #5

Assessment of the Comparative Productive Performance of Three Solar PV Technologies Installed at UQ Gatton Campus Using the NREL SAM Model

Prepared by Phillip Wild, PhD
Postdoctoral Research Fellow
Global Change Institute
The University of Queensland

Assessment of the Comparative Productive Performance of Three Solar PV Technologies Installed at UQ Gatton Campus Using The NREL SAM Model

By Phillip Wild
Email: p.wild@uq.edu.au
Telephone: work (07) 3346 1004; Mobile 0412 443 523
Version 4 – 15 June 2016

Abstract

The economic assessment of the viability of different types of solar PV tracking technologies centres on assessment of whether the annual production of the different tracking technologies is increased enough to compensate for the higher cost of installation and operational expenditures incurred by the tracking systems. To investigate this issue, we use the NREL's SAM model to simulate electricity production from three representative solar PV systems installed at Gatton. In these simulations we use hourly solar irradiance, weather and surface albedo data, technical data relating to both module and inverter characteristics and impacts associated with module soiling and near-object shading. A key finding was that over the period 2007 to 2015, average increases in annual production of between 23.9 and 24.3 per cent and 38.0 and 39.1 per cent were obtained for Single Axis and Dual Axis tracking systems relative to the Fixed Tilt system.

(1) Introduction

The economics of solar PV has changed significantly over the last decade with installation costs declining significantly following the marked take-up of solar PV systems, often on the back of generous Government feed-in tariff support particularly in Europe. More recently, a marked increase in the up-take of roof-top solar PV occurred in Australia on the back of generous state-based Feed-in tariffs and the Federal Government's renewable energy target, and, more recently, the small scale renewable energy target (RMI, 2014).

Unlike the case in particularly Spain and Germany, however, there were no equivalent feed-in tariffs available for large scale investments in Australia, and these types of investments have been much slower to emerge.

To-date, investment in large commercial and industrial scale solar PV projects has largely proceeded on the basis of support from two particular programs: (1) Australian Capital Territory (ACT) reverse auction for solar PV projects (ACT, 2016); and (2) Government support from the Australian Renewable Energy Agency (ARENA, 2016), in conjunction with financial support from the Clean Energy Finance Corporation (CEFC) for larger projects (CEFC, 2016). This has occurred against a general backdrop of a concerted attack on renewable energy in Australia since late 2013. Moreover, policy and regulatory uncertainty accompanying this attack has led to a general drying up of investment in large-scale renewable energy projects with major retail electricity companies now appearing unwilling to enter Power Purchase Agreement (PPA) agreements traditionally needed to secure private sector finance for projects. This has led to the situation whereby the required capacity to meet the 2017 Large Scale Renewable Energy Target (LRET) now appears to be in excess of 3000 MW's in arrears (Green Energy Markets, 2015).

The structure of this paper is as follows. The next section will give a brief description of the solar array at the University of Queensland's (UQ) Gatton Campus that underpins the modelling performed for this paper. Section (3) will contain a discussion of critical aspects affecting the comparative assessment of the production of representative technologies contained in the solar array under investigation. This will include an outline the modelling employed in the paper to generate solar PV yield and discussion of the results of the modelling relating to production and annual capacity factor (ACF) outcomes, respectively. Section 4 will contain conclusions.

(2) University of Queensland Gatton Solar Research Facility (GSRF)

The GSRF was funded under the Federal Government's Education Investment Fund (EIF) scheme ($40.7M), and was part of the larger ARENA funded project Australian Gas and Light Pty Ltd (AGL) Nyngan and Broken Hill Solar farms (UQ, 2015a). These two solar PV farms have a capacity of 102 MW and 53 MW, respectively. The total cost of the combined project was $439.08 million, of which ARENA contributed $166.7 million and the New South Wales

State Government $64.9 million (AGL, 2015). The objective of the EIF Project was to act as a pilot for the utility-scale plants – proofing technology and establishing supply chains.

The GSRF solar array installed at Gatton is a 3.275 megawatt pilot plant that comprises three different solar array technologies: (1) a Fixed Tilt (FT) array comprising three identical 630 kW systems (UQ, 2015b); (2) a 630 kW Horizontal Single Axis Tracking (SAT) Array utilising First Solar's SAT system (UQ, 2015c); and (3) a 630 kW Dual Axis Tracker (DAT) utilising the Degertraker 5000 HD system (UQ, 2015d). A good overview of the principals underpinning sun-tracking methods can be found in Mousazadeh et al. (2009).

An overhead NearMap picture of the Gatton array is contained in Figure 1. The FT system design at Gatton has the following technical design features: (1) all modules have a tilt angle of 20 degrees; (2) all modules have an azimuth angle of 357 degrees (e.g. modules are facing in the direction of three degrees west of north). The three FT arrays have a combined total of 21, 600 modules. These arrays can be located, respectively, at the top right hand side (termed the 'top' FT array) and with the main FT array being located just below the buildings and line of trees but above the road in Figure 1.

The SAT array at Gatton has the following technical aspects: (1) the array is a horizontal array and thus has a tilt angle of 0 degrees; (2) the array has an azimuth angle of 357 degrees (e.g. same as the FT system); (3) maximum tracker rotation limit is set to 45 degrees; and (4) no backtracking is implemented. Backtracking is a control procedure that is used in some SAT systems to minimise the degree of self-shading from nearby SAT trackers. The total number of modules in the SAT array is 7,200 modules with 120 individual SAT tracking systems. The SAT array can be located in Figure 1 immediately below the top FT array, adjacent to the main FT array and also above the road in Figure 1.

The third array is the DAT array. There are 160 individual trackers installed at Gatton that are capable of a 340 degree slewing motion and a 180 degree tilt that allow the modules to directly face the sun at all times of the day, thereby maximising output (UQ 2015d). As in the case of the SAT system, the DAT system also has 7,200 modules in total. In Figure 1, the DAT array is located underneath the main FT array and below the road.

Figure 1. NearMap Picture of the UQ Gatton Solar Array

The same type of modules are installed on all three solar array technologies located at Gatton – First Solar FS-395 PLUS (95 W) modules. The same type of inverter is also installed with each of the 630 kW systems – SMA Sunny Central 720CP XT inverters. The three FT sub-arrays are connected to three inverters while the SAT and DAT sub-arrays are connected to a single inverter each. Hence, the whole array contains five inverters. Moreover, through the connection agreement with Energex, each inverter's output is currently limited to 630 kW.

In this paper we will restrict attention to a comparative assessment of the production results of three representative 630 kW FT, SAT and DAT sub-arrays. This will involve assessing the output performance of the SAT and DAT sub-arrays and the left hand side sub-array of the main FT array installed at Gatton – e.g. the left most FT sub-array.

(3) Comparative Assessment of Production Outcomes of the Three Representative Arrays at Gatton.

Economic assessment of the viability of different types of solar PV tracking technologies typically centres on an assessment of whether the annual production of the different tracking technologies is lifted enough relative to the benchmark FT system in order to compensate for the higher installation and operational costs incurred by the tracking systems. The installation costs refer to the 'overnight' ($/Wp) or equivalently ($/kW) installation costs that would be incurred if the whole solar PV plant could be constructed overnight. This expenditure category would include costs associated with the purchase of modules and inverters as well as various categories of balance of plant costs. The latter component would include expenditures associated with: (1) costs of transport to site; (2) site preparation, racking and mounting activities; (3) DC and AC electrical connection; and (4) other non-production activity such as insurance costs, administration and connection licensing (RMI, 2014).

The second cost component is operational costs, in particular, Operational and Maintenance (O&M) expenditures associated with keeping modules and inverters operating efficiently. For tracking systems, additional O&M costs would also have to be levied against the need to also keep the tracking infrastructure working efficiently. In general, solar tracking systems include a tracking device, tracking algorithm, control unit, positioning system, driving mechanism and sensing devices.

Large optical errors in tracking the sun's position will result in potentially large reductions in electricity generated from the PV system relative to what would have been obtained if the tracking mechanism was working properly. A crucial question, however, is how large is how large? Mousazadeh et al. (2009) point out that trackers do not need to be pointed directly at the sun to be effective. They argued that if the aim is off by 10 degrees implying an optical tracking error of 10 degrees, the output will still be 98.5% of the full-tracking maximum. Stafford et al. (2009) report that tracking errors may not be negligible when compared with typical system acceptance angles – the maximum pointing error that the PV system can tolerate without a substantial loss of power output. They also found that the fraction of available energy captured tended to decline with the degree of the system's acceptance angle, whilst increasing with the degree of the acceptance angle. Additional support for this broad finding is also cited in (Sallaberry et al, 2015a, p. 195). However, complicating this issue is the observation in Stafford et al (2009) that different solar technologies such as High Concentration Photovoltaic (HCPV), Low Concentration Photovoltaic (LCPV), Concentrated Solar Thermal (CSP) and single- and dual-axis tracked flat-plate PV panels all have different relationships between generated power and tracking error, leading to different tracking requirements for each technology.

If large reductions in output arise because of the presence of large optical tracking errors relative to the system's acceptance angle, this would impair the economic viability of the tracking system. Some electricity must also be consumed internally by the system in order to operate the motors that drive the shifts in position of one or more of the axes associated with the particular tracking mechanism. This internal electricity consumption is typically netted of the gross output produced by the system when tracking is operating during the day.

Thus, O&M expenses are likely to be directly proportional to the complexity of the tracking system employed. As such, O&M provisions associated with more complex two axis trackers such as the DAT system are likely to be of a higher magnitude because the tracking infrastructure is more complex and larger in scale and is, therefore, more likely to be prone to mechanical faults or break-downs.

(3.1) Assessment of System Output Using National Renewable Energy Laboratory (NREL) System Advisor Model (SAM)

The SAM model, developed by NREL, was used to simulate electricity production of the three representative solar PV systems installed at Gatton. To run simulations in SAM, various user supplied inputs are required. These relate to: (1) hourly solar and weather data; (2) technical information about modules, inverters and array sizing and design; (3) soiling effects; (4) shading effects; and (5) DC and AC electrical losses. In the modelling performed for this paper, we also assumed that all modules, inverters and tracking infrastructure were in good working order throughout the SAM simulations.

Solar and weather data

The solar and weather data are stored in a SAM CSV weather file which contains information on the solar PV site's latitude, longitude, elevation and time zone (Gilman, 2015, Ch. 3). The solar data included in the file relates to Global Horizontal Irradiance (GHI), Direct Normal Irradiance (DNI) and Diffuse Horizontal Irradiance (DHI). There is an option in SAM for the software to internally calculate DHI using internal calculations of the sun's position by the software given the latitude, longitude, elevation of the site and commencing date and time of the simulation. This option was utilised in the simulations underpinning the results reported in this paper. The Perez Sky Diffuse model is also used to determine Plane-of-Array (POA) irradiance (Gilman, 2015, Section 6.2).

The GHI and DNI data used in the simulations were obtained from the Australian Bureau of Meteorology's (BOM) hourly solar irradiance gridded data (BOM, 2015). The actual DHI data included in the SAM CSV weather files were calculated from the following equation:

$$DHI = GHI - DNI \times \cos(sun\_zenith\_angle), \tag{1}$$

after determining the sun's position and zenith angle according to the algorithm in Reda and Andreas (2003). However, recall that the SAM model calculates the sun's position internally and the actual DHI data used in the simulations was also calculated internally by SAM, over-writing the DHI data included originally in the weather file.

The climate data required by the SAM model included both ambient and dew point temperature (degrees Celsius), relative humidity (percentage), mean sea level pressure (MSLP in hectopascals), wind speed (meters per second) and wind direction (degree east of north). This data was sourced from the BOM's Automatic Weather Station (AWS) located at the University of Queensland campus at Gatton. This data was supplemented by MSLP pressure data from the BOM's Amberley and Toowoomba weather stations because they were not available for Gatton. Gatton pressure was calculated by the relation:

$$Gatton\_MSLP = Toowoomba\_MSLP + [0.105075 \times (Amberley\_MSLP - Toowoomba\_MSLP)], \tag{2}$$

with the coefficient '0.105075' reflecting the fact that pressure changes with elevation. Thus we include an additional adjustment to the Amberley MSLP value to reflect the fact that Gatton has a higher elevation than Amberley but is much closer in elevation to Amberley than to Toowoomba. For example, Gatton has an elevation of 89 meters, Amberley 24.2 meters and Toowoomba 640.9 meters. Given these elevation levels, the coefficient '0.105075' used in equation (2) was calculated as the ratio of the difference in elevation between Gatton and Amberley and the difference in elevation between Toowoomba and Amberley, that is, as (89-24.2)/(640.9-24.2).

It should also be noted that only the ambient temperature and wind speed data are actually used by SAM in modelling solar PV yield. However, the SAM model requires the other data to be included in the weather file otherwise the program will not run. Finally, we also include in the SAM CSV weather file data for snow cover (set to zero) and surface albedo. The surface albedo data was compiled from MODIS White Sky Albedo data (NASA, 2015). This was taken from representative two weekly samples taken at the Gatton latitude and longitude coordinates to reflect differences in both season and ENSO cycle status. Specifically, averages of MODIS white albedo readings were obtained for the list of dates in Table 1.

Table1. Dates used to estimate surface albedo at Gatton by season and ENSO Status

Season	La Nina	ENSO Neutral	El Nino
Summer	9-24 January 2009	11-26 December 2013	10-26 December 2009
Autumn	7-22 April 2010	7-22 April 2013	7-22 April 2006
Winter	2-17 June 2010	10-25 June 2013	10-25 June 2006
Spring	8-23 October 2010	16-31 October 2013	16-31 October 2009

Module, inverter and solar array design

Data is also required about the technical characteristics of the modules and inverters used at Gatton. As mentioned above, the modules used are First Solar FS-395 PLUS (95 W) modules while the inverters are SMA Sunny Central 720CP XT inverters. Sets of technical parameters from First Solar and SMA's product data sheets for the modules and inverters were required for the specific module and inverter models used in the SAM modelling. In the case of the modules, the model used in the SAM simulations was the 'California Energy Commission (CEC) Performance Model with User Entered Specifications' option (Gilman, 2015, Ch. 9.5). The technical parameters required by this model and the values used in the SAM simulations are listed in Appendix A, Panel (A). This option makes use of a coefficient calculator developed in Dobos (2012) to calculate the model parameters required by the CEC model from standard module specifications provided on manufacturer's data sheets. This model also uses the NOCT cell temperature model to model cell temperatures (Gilman, 2015, Ch. 9.7).

The option used to model the inverter was the 'Inverter Datasheet' implementation of the Sandia Inverter Model (Gilman, 2015, Ch. 11.2) with the technical parameters and the values used in the SAM simulations listed in Appendix A, Panel (B). Recall that for each of the three FT, SAT and DAT systems modelled, 7200 modules and a single inverter was used, with the inverter's AC output constrained to 630 kWac in each case.

Implementation of SAM modelling also required data relating to system design features. In the design and sizing of the array, the most crucial information is: (1) number of modules in a string; (2) number of strings in parallel; and (3) number of inverters. From this information as well as from the additional information relating to both modules and inverters, the following system information is determined: (1) maximum DC capacity of the solar array; (2) maximum DC input capacity of the inverters; and (3) maximum AC output capacity of the inverters. The key system design parameters and quantities used in the SAM simulations are reported in Panel © of Appendix A.

Soiling effects

In order to calculate the various system-wide capacity limits and running simulations in SAM, account needs to be taken of module soiling (Gilman, 2015, Ch. 7.5). It is generally accepted that after solar irradiance and air temperature, module soiling will be the next most crucial issue affecting solar PV yield. Four different soiling rate assumptions were employed in the modelling for the paper. These relate to low, medium and high soiling scenarios and additionally, a soiling scenario based upon recommendations of First Solar (ARUP, 2015).

All soiling scenarios are based upon consideration of recorded daily rainfall over the period 2007 to 2015. The rainfall data utilised in constructing the various soiling scenarios is that recorded at the UQ Gatton Campus BOM AWS located within two kilometres of the solar farm. The mean average monthly rainfall for this site is presented in Figure 2. This figure clearly shows a wet season encompassing the period November to March and a dry season arising over the period April to September with a transition period between these two seasons occurring in October.

In determining monthly soiling rates, it was assumed that 25 millimetres (mm) or more of rainfall during a particular day in a month would be sufficient to restore the modules to their ‘pristine’ condition associated with their commissioning. During the wet season, it was common to have some days with a couple of inches of rainfall and multiple days with over an inch of rainfall. Similarly, it was assumed that daily rainfall totals of less than 5 mm was not sufficient to engender any cleansing of the modules. Relatively small amounts of cleaning were assumed for daily rainfall totals of between 5 mm and 10 mm, relating to reduced accumulative soiling within a month of 20%. More moderate cleansing power for daily rainfall totals of between 10 mm and 16 mm were assumed that reduced accumulated soiling within a month by 50%. Finally, for daily rainfall totals between 17 mm and 25 mm, it was assumed that accumulated soiling within a month was reduced by 80%.

Figure 2. Mean average rainfall at UQ Gatton Campus BOM AWS

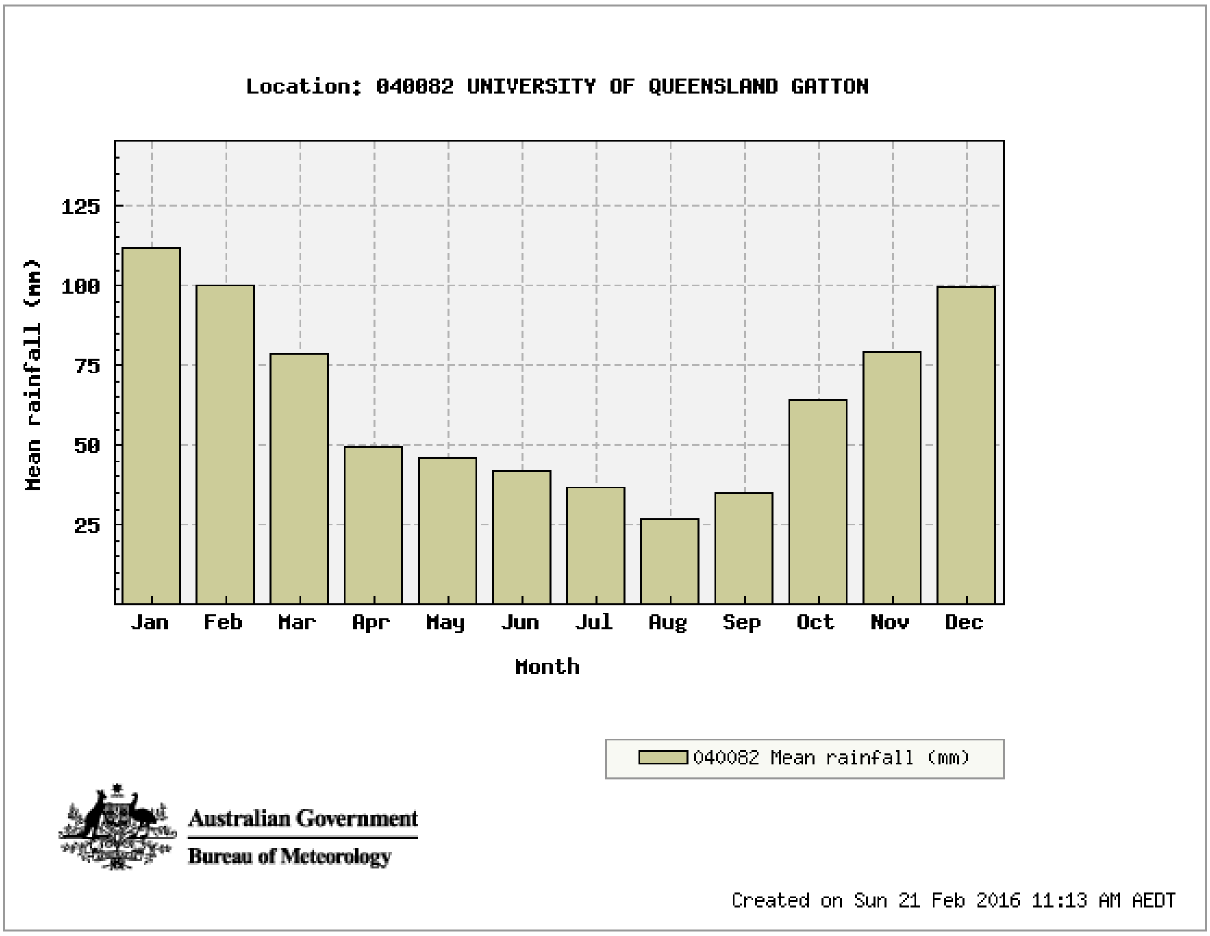

The accumulative soiling was calculated from the monthly rainfall totals recorded for the UQ Gatton Campus BOM AWS for two different daily soiling rates assumptions associated with daily rainfall totals within each month that was less than or equal to 5 mm. The low soiling scenario assumed a daily growth in soiling effect of 0.033% per day. The medium soiling scenario assumed a higher daily soiling rate of 0.11% per day. It should be noted that the daily soiling rate of 0.11% per day was adopted from (Kimber et al, 2006) who estimated this daily soiling rate for rural areas in Central Valley and Northern California – for example, see Figure 3 of (Kimber et al, 2006). Assuming a 30 day month, these two daily soiling rates would produce monthly soiling rates of 1.0 and 3.3 per cent, respectively. To the extent that consecutive months had no rainfall (defined as less than or equal to 5 mm per day), these monthly soiling rates would be added together over time producing monthly soiling rates that could significantly exceed 1.0 and 3.3 per cent.

If daily rainfall exceeded 25 mm during the month, total module cleansing was assumed with the monthly soiling rate being set back to the assumed ‘pristine’ commissioning rate of 1.0 per cent. If one or more of the daily rainfall totals during the month was between 5 mm and 10 mm, 80 per cent of the assumed within month soiling rate was added on to the previous months soiling rate thus indicating some marginal cleansing effect on the modules. If one or more of the daily rainfall totals was between 10 mm and 16 mm, 50 per cent of the assumed within monthly soiling rate was added onto the previous months soiling rate, indicating some partial cleansing effect on the modules. If one or more of the daily rainfall totals fell between 17 mm and 25 mm, only 20 per cent of the assumed within monthly soiling rate was added onto the previous months soiling rate. Thus the main effect of daily rainfall less than 25 mm is to offset some of the accumulated within month soiling effect with the larger impacts being associated with daily rainfall rates of between 17 mm and 25 mm.

For completeness, a fourth soiling scenario is also employed, based on an approach recommended by First Solar (ARUP, 2015, Section 4.2.1.3). This approach involves assuming a monthly soiling rate of 3.0 per cent if monthly rainfall was less than 20 mm, 2.0 per cent if monthly rainfall was between 20 mm and 50 mm and 1.0 per cent if the monthly rainfall was greater than 50 mm.

The monthly soiling rates were also corrected for local spectrum following the method advocated in First Solar (2015). This correction is based upon the fact that modules are rated under Standard Test Conditions assuming a spectral distribution as defined by ASTM G173 for an air mass of 1.5. However, site-specific spectral irradiance will typically deviate from STC resulting in varying performance in regard to module nameplate capacity.

First Solar proposed a method to account for that type of difference based upon a new variable termed a spectral shift factor, which was driven principally by the amount of precipitable water in the atmosphere. Further, they proposed a method for estimating a time series of the amount of precipitable water in the atmosphere at a site’s location from the time series of relative humidity and ambient temperature at the site. These hourly spectral shift factors are subsequently expressed as aggregate monthly spectral shift factors by first weighting the hourly factors by hourly solar irradiance (GHI) data and then averaging over each calendar month. These variables can then be viewed as a relative loss or gain with respect to nominal energy with positive values depicting a loss in energy due to local spectrum whilst negative values denote an energy gain due to local spectrum.

In accordance with the approach outlined in First Solar (2015), the monthly spectral shift factors are implemented by combining them with the monthly soiling loss factors to obtain an ‘augmented’ monthly soiling loss factor. In this context, a negative average monthly spectral loss factor would reduce the augmented soiling loss factor while a positive average monthly spectral loss factor would increase the augmented soiling loss factor. This outcome is consistent with our expectations because a positive average monthly spectral loss factors represent a *loss* in energy and which is subsequently applied as an increase in the original soiling loss factor. On the other hand, a negative average monthly spectral loss factor denotes a *gain* in energy and is subsequently applied as a reduction in the original soiling loss factor.

The set of augmented monthly soiling loss factors for the four soiling scenarios considered are reported in Table 2. It should be noted that in calculating the augmented soiling losses, if the energy gain exceeded the original calculated soiling loss, the augmented soiling loss would become negative. In such cases, the absolute value of the smallest negative monthly augmented soiling loss was calculated and added to each average monthly augmented soiling loss factor to ensure that they were all non-negative. To offset this operation, this absolute value was similarly subtracted from one or more of the DC loss factors to ensure a zero net change in loss factors. These subtractions were typically applied to DC mismatch and nameplate loss categories.

Inspection of Table 2 indicates that the lowest augmented soiling losses occur during the wet season November to March reflecting both the additional cleansing power of higher rainfall totals as well as energy gains associated with local spectrum over these particular months. The values of zero in January point to this month containing the smallest negative augmented soiling factor losses originally, and whose absolute values were subsequently added to each monthly value to ensure that the augmented monthly soiling loss factors were all non-negative.

The ‘Low’, ‘Medium’ and ‘First Solar’ soiling scenarios were discussed above. The ‘High’ soiling scenario was calculated from the data derived under the medium scenario that utilised a daily soiling growth rate of 0.11% per day. These values produced monthly values over each month for years 2007 to 2015. The Medium soiling scenario was simply calculated as the average of that data on a month-by-month basis. Similarly, the High soiling scenario was calculated as the 90th percentile of that data, on a month-by-month basis.

It is clear from Table 2 that the Low and First Solar soiling scenarios produce very similar results with annualised averages of 1.7 and 1.8 per cent, respectively. The maximum soiling rates occur in the July to September time period in the range of 3.2 to 3.8 per cent whilst the lowest soiling rates occur in the December to March time frame in the range of 0.0 to 0.3 and 0.0 to 0.7 per cent, respectively. Because of this observed closeness, we will only report the results associated with the 'Low' soiling scenario as the generic low soiling scenario to be considered further in the paper.

In the case of the Medium soiling scenario, an annualised average of 3.2 per cent was obtained. Once again, the maximum and minimum soiling rates appear in the July to September and December to March time periods in the range of 6.6 to 7.0 per cent and 0.0 to 0.5 per cent, respectively. The results associated with the High soiling scenario denote more significant increases in both maximum and minimum soiling rates under this scenario although the periods when these rates arise continues to remain the same. Specifically, the maximum monthly augmented soiling rates are now in the range of 9.5 to 12.5 per cent while the minimum rates are in the range of 0.0 to 1.8 per cent. The annualised average for this particular scenario is 5.7 per cent.

Table2. Different augmented soiling rate configurations (Percentage)

Month	Low	Medium	High	First Solar Rates
Jan	0.0	0.0	0.0	0.0
Feb	0.1	0.5	1.8	0.4
Mar	0.3	0.5	1.1	0.7
Apr	1.2	2.0	4.3	1.5
May	2.3	4.4	8.2	2.6
Jun	2.4	4.0	6.7	2.7
Jul	3.6	7.0	9.5	3.8
Aug	3.7	6.8	10.6	3.5
Sep	3.2	6.6	12.5	3.2
Oct	2.5	5.2	10.5	2.3
Nov	0.9	1.4	2.5	0.9
Dec	0.3	0.4	0.9	0.3
Average	1.7	3.2	5.7	1.8

Shading effects

Solar PV yield assessment using SAM also requires that the effects of shading on modules be accounted for. We employed SAM's 3d shading calculator to determine near-object shading effects. Near-object shading can be interpreted as a reduction in POA incident irradiation by external objects located near to the array such as building, hills and trees and is assumed to affect each sub-array uniformly. This is performed in SAM utilizing a three-dimensional representation of the sub-arrays and nearby external objects. Near-object shading affects both direct (beam) and diffuse POA irradiance (Gilman, 2015, Ch. 7.2).

In SAM, the reduction in beam irradiance due to near-object shading is modelled by a set of hourly shading losses that reduce the plane-of-array beam solar irradiance in a given hour. The reduction in diffuse POA irradiance is modelled by a single sky diffuse loss percentage. In calculating the sky diffuse shading factor, an isotropic diffuse radiation model is assumed in which diffuse radiation is assumed to be uniformly distributed across the sky. Because this component does not depend upon the position of the sun, but only on the system geometry, it is constant over the whole year (Gilman, 2015, Ch. 7.2).

We utilised SAM's 3d calculator to determine both near object direct beam and constant sky diffuse shading losses for the three representative arrays. The constant sky diffuse shading losses for the three representative arrays are reported in the last row of Panel (D), Appendix A and are 4.45, 1.96 and 1.1 per cent, respectively, for the representative FT, SAT and DAT arrays.

The near object direct beam shading losses determined for the three representative arrays are documented in Table 3, Panels (A), (B) and (C) for the FT, SAT and DAT arrays. It should be noted that in all three panels, the values of 100 per cent that are shaded in red represent periods with complete shading. These arise in the early morning and early evening hours, with some further constriction to operational hours also arising in winter relative to summer. Values of zero indicate no shading impacts and partial near object shading effects are represented by values between zero and 100, with larger impacts associated with higher magnitude values.

In general, the DAT array (Panel C) has the lowest shading impacts in the early morning and early evening hours when compared to the shading effects on both the FT and SAT arrays. The SAT array has the next lowest shading impacts with the FT array experiencing the highest near object shading effects. Note that this outcome was also observed in the constant shy diffuse shading loss percentages reported above. Of particular interest for PV yields projections is that the representative FT array experiences very little or no near-object direct beam shading over the period 9 AM to 2 PM. In contrast, the representative SAT and DAT arrays experience very little or no near-object direct beam shading over slightly broader time horizons of 8 AM to 3 PM and 7 AM to 4 PM, respectively.

Table3. Direct beam near-object shading factors for Gatton arrays (Percentage)

Panel (A): Direct beam shading factors: representative FT array

Month	5:00 AM	6:00 AM	7:00 AM	8:00 AM	9:00 AM	10:00 AM	11:00 AM	12:00 PM	1:00 PM	2:00 PM	3:00 PM	4:00 PM	5:00 PM	6:00 PM
JAN	100	0.0	0.0	0.0	0.0	0.0	0.0	0.0	0.0	0.0	0.0	0.0	0.0	100
FEB	100	0.0	0.0	0.0	0.0	0.0	0.0	0.0	0.0	0.0	0.0	0.0	0.0	100
MAR	100	0.0	0.0	0.0	0.0	0.0	0.0	0.0	0.0	0.0	0.0	0.0	0.0	100
APR	100	11.7	0.0	0.0	0.0	0.0	0.0	0.0	0.0	0.0	0.0	0.0	67.0	100
MAY	100	83.5	4.7	0.0	0.0	0.0	0.0	0.0	0.0	0.0	0.6	36.5	100	100
JUN	100	100	39.6	1.2	0.0	0.0	0.0	0.0	0.0	0.1	3.9	56.1	100	100
JUL	100	100	33.6	0.6	0.0	0.0	0.0	0.0	0.0	0.0	1.3	42.3	100	100
AUG	100	94.7	0.1	0.0	0.0	0.0	0.0	0.0	0.0	0.0	0.0	2.8	100	100
SEP	100	0.0	0.0	0.0	0.0	0.0	0.0	0.0	0.0	0.0	0.0	0.0	14.7	100
OCT	100	0.0	0.0	0.0	0.0	0.0	0.0	0.0	0.0	0.0	0.0	0.0	0.0	100
NOV	0.0	0.0	0.0	0.0	0.0	0.0	0.0	0.0	0.0	0.0	0.0	0.0	0.0	100
DEC	100	0.0	0.0	0.0	0.0	0.0	0.0	0.0	0.0	0.0	0.0	0.0	0.0	100

Panel (B): Direct beam shading factors: representative SAT array

Month	5:00 AM	6:00 AM	7:00 AM	8:00 AM	9:00 AM	10:00 AM	11:00 AM	12:00 PM	1:00 PM	2:00 PM	3:00 PM	4:00 PM	5:00 PM	6:00 PM
JAN	3.5	0.0	0.0	0.0	0.0	0.0	0.0	0.0	0.0	0.0	0.0	0.0	0.0	5.2
FEB	100	0.0	0.0	0.0	0.0	0.0	0.0	0.0	0.0	0.0	0.0	0.0	0.0	3.6
MAR	100	0.0	0.0	0.0	0.0	0.0	0.0	0.0	0.0	0.0	0.0	0.0	0.0	100
APR	100	0.0	0.0	0.0	0.0	0.0	0.0	0.0	0.0	0.0	0.0	0.0	39.7	100
MAY	100	5.3	0.0	0.0	0.0	0.0	0.0	0.0	0.0	0.0	0.0	34.2	100	100
JUN	100	100	8.8	0.0	0.0	0.0	0.0	0.0	0.0	0.0	0.5	53.2	100	100
JUL	100	100	5.1	0.0	0.0	0.0	0.0	0.0	0.0	0.0	0.0	31.5	100	100
AUG	100	0.7	0.0	0.0	0.0	0.0	0.0	0.0	0.0	0.0	0.0	1.4	100	100
SEP	100	0.0	0.0	0.0	0.0	0.0	0.0	0.0	0.0	0.0	0.0	0.0	32.4	100
OCT	0.8	0.0	0.0	0.0	0.0	0.0	0.0	0.0	0.0	0.0	0.0	0.0	0.0	100
NOV	0.0	0.0	0.0	0.0	0.0	0.0	0.0	0.0	0.0	0.0	0.0	0.0	0.0	100
DEC	0.1	0.0	0.0	0.0	0.0	0.0	0.0	0.0	0.0	0.0	0.0	0.0	0.0	10.9

Panel (C): Direct beam shading factors: representative DAT sub-array

Month	5:00 AM	6:00 AM	7:00 AM	8:00 AM	9:00 AM	10:00 AM	11:00 AM	12:00 PM	1:00 PM	2:00 PM	3:00 PM	4:00 PM	5:00 PM	6:00 PM
JAN	8.8	2.2	0.7	0.2	0.0	0.0	0.0	0.0	0.0	0.0	0.0	0.0	0.0	0.0
FEB	100	3.1	0.8	0.0	0.0	0.0	0.0	0.0	0.0	0.0	0.0	0.0	0.0	0.0
MAR	100	2.5	0.0	0.0	0.0	0.0	0.0	0.0	0.0	0.0	0.0	0.0	0.0	100
APR	100	5.6	0.0	0.0	0.0	0.0	0.0	0.0	0.0	0.0	0.0	0.0	0.0	100
MAY	100	15.1	0.0	0.0	0.0	0.0	0.0	0.0	0.0	0.0	0.0	0.0	100	100
JUN	100	100	0.0	0.0	0.0	0.0	0.0	0.0	0.0	0.0	0.0	0.0	100	100
JUL	100	100	0.0	0.0	0.0	0.0	0.0	0.0	0.0	0.0	0.0	0.0	100	100
AUG	100	13.6	0.0	0.0	0.0	0.0	0.0	0.0	0.0	0.0	0.0	0.0	100	100
SEP	100	0.0	0.0	0.0	0.0	0.0	0.0	0.0	0.0	0.0	0.0	0.0	0.0	100
OCT	5.0	1.7	0.0	0.0	0.0	0.0	0.0	0.0	0.0	0.0	0.0	0.0	0.0	100
NOV	7.5	1.5	0.5	0.0	0.0	0.0	0.0	0.0	0.0	0.0	0.0	0.0	0.0	100
DEC	7.8	1.8	0.6	0.0	0.0	0.0	0.0	0.0	0.0	0.0	0.0	0.0	0.0	0.0

It should be noted that in the simulations performed for this paper, we did not include any self-shading effects because such effects are not calculated for the DAT systems in the most current version of SAM. However, SAM does calculate self-shading losses for both FT and SAT arrays and other research indicates average self-shading losses of a tenth of one per cent for the representative FT array and one per cent for the representative SAT array (Gilman, 2015, Ch. 7.3).

The reason why self-shading losses are greater for the SAT array is that it can rotate to track the azimuth angle of the sun, thereby producing greater yield in the early morning and early evening hours when self-shading effects are most prevalent. Thus, the reduction in output due to self-shading is subsequently greater in the case of SAT array when compared with the FT array whose azimuth (and tilt) angle are fixed throughout the day and the system cannot track the sun's position.

In general, this outcome would be expected to be magnified further in the case of the DAT array whose tilt and azimuth angles can track the sun's zenith and azimuth angles over the day, thus being more susceptible to potentially larger output reductions in early morning and evening hours because of self-shading effects than in the case of the SAT array. However, potentially moderating this effect is the fact that the DAT trackers are located further apart than the rows of FT and SAT arrays. In modelling self-shading, the row spacing between the rows of the FT arrays were determined to be 4.3 meters while the equivalent spacing for the SAT array was determined to be 7.3 meters. In contrast, the shortest distance between individual DAT trackers was determined to be around 10.5 meters on a diagonal orientation and around 20.6 meters using a vertical orientation. More generally, the investigation and quantifying of self-shading impacts (including ground reflected shading) on the solar PV yield of the three technologies installed at GSRF is an ongoing research programme.

DC and AC electrical losses

We have also adopted the following values for derating DC array output associated with DC electrical losses of between 3.56 and 3.99 per cent, depending upon the array technology and AC electrical losses of 2.14 per cent. Details of specific settings are listed in Appendix A, Panel (D). It should be recalled that the DC 'Mismatch' and 'Nameplate' loss factors were partially reduced to ensure that net losses were zero when the modification were made to ensure that the augmented soiling loss factors adjusted for local spectrum were non-negative. More information about typical loss factor settings for Solar PV simulations can be found in Thevenard et al (2010), Tapia Hinojosa (2014) and ARUP (2015, Section 4.2).

(3.2) Assessment of Simulated Annual Production Levels of the Different Representative Solar PV Arrays

Once all the required inputs have been made available to SAM, simulations can be performed to assess the production outcomes of each representative solar PV technology. The production results from the SAM modelling are reported in Table 4, Panels (A), (B) and (C) for the low, medium and high soiling scenarios.

Given the focus in economic viability studies on revenue earnt from electricity supplied directly to the grid, we calculate annual electricity production but exclude any electricity used internally by the system at night which is represented as a negative output in the annual production figures compiled by SAM. We calculate the annual production levels by aggregating the hourly system output after zeroing out any negative hourly production entries associated with internal consumption of electricity by the system at night. Thus, this production concept reflects an energy sent-out production concept, that is, the electricity exported to the grid during the day that is available to earn revenue by servicing demand.

Two particular revenue streams are envisaged. The first is revenue attributed to the solar array associated with reduction in grid off-take of electricity which is subsequently replaced by electricity produced by the solar array. The second revenue stream is revenue from the sale of Large-Scale Generation Certificates (LGC) through the production of eligible renewable energy under the Australian Government's Large-Scale Renewable Energy Target (LRET) scheme (CER, 2016).

The second last row of each panel of Table 4 contains the average production levels whilst the last row in each panel contains aggregate total production results calculated for each representative array compiled from the results listed above for the period 2007 to 2015. Assessment of all panels of Table 4 indicates considerable year-on-year variation. Of particular note is the sizable reduction in 2010, in relative terms, corresponding to the onset of a severe La Nina, especially over the second half of 2010, culminating in the significant flooding event in South East Queensland in January 2011. Relatively higher production totals were also recorded in 2007 and 2012-2014 when coming out of relatively weak El Nino and sustained La Nina patterns, respectively. The production levels, on the whole, are largest in magnitude in 2014, reflecting the onset of ENSO neutral conditions but with a strongly emerging El Nino bias. Interestingly, however, a reduction in annual production arises in 2015, relative to 2013-2014, accompanying the formal move to severe El Nino conditions in 2015.

Table4. Production Totals by Array Type and Soiling Scenario

Panel (A): Low soiling rates

Year	FT	SAT	DAT
2007	1197.1	1491.4	1661.7
2008	1170.5	1459.9	1623.2
2009	1180.3	1468.8	1644.8
2010	1061.3	1298.6	1446.6
2011	1138.0	1401.5	1567.6
2012	1196.7	1491.5	1658.0
2013	1229.3	1548.1	1711.2
2014	1252.2	1563.2	1747.1
2015	1196.5	1442.2	1598.7
Average	1180.2	1462.8	1628.8
Total	10621.8	13165.1	14659.0

Panel (B): Medium soiling rates

Year	FT	SAT	DAT
2007	1179.8	1472.0	1643.3
2008	1153.6	1440.8	1605.7
2009	1162.4	1448.5	1625.4

2010	1046.2	1281.3	1430.3
2011	1121.5	1382.7	1549.6
2012	1179.8	1472.3	1637.7
2013	1211.7	1528.3	1693.2
2014	1234.2	1543.0	1727.9
2015	1179.7	1424.6	1582.5
Average	1163.2	1443.7	1610.6
Total	10468.9	12993.6	14495.6

Panel (C): High soiling rates

Year	FT	SAT	DAT
2007	1151.3	1438.9	1610.8
2008	1125.3	1408.3	1574.1
2009	1133.1	1414.8	1591.9
2010	1021.1	1252.3	1401.6
2011	1094.3	1351.2	1518.0
2012	1151.4	1439.6	1603.1
2013	1182.2	1494.2	1660.6
2014	1204.3	1508.6	1693.5
2015	1151.8	1394.2	1553.4
Average	1135.0	1411.4	1578.6
Total	10214.7	12702.2	14207.1

The system-wide impacts of soiling can also be discerned from Table 4. Under the low soiling scenario, average annual production levels of 1180.2, 1462.8 and 1628.8 MWh were reported in Panel (A) for the representative FT, SAT and DAT arrays, respectively. Similarly, total production values for the period 2007 to 2015 of 10621.8, 13165.1 and 14659.0 MWh were also recorded. Comparison of these production results with the equivalent values associated with the medium and high soiling scenarios point to reductions in both average annual and total production for all three representative arrays. Furthermore, the rate of reduction in average annual and total production relative to the low soiling scenario increases with the level of soiling.

Specifically, for the representative FT array, average annual production was reduced by 1.4 and 3.8 per cent, relative to the low soiling scenario's average annual production level cited above. For the representative SAT array, the equivalent reduction in annual average production was 1.3 and 3.5 per cent, respectively. In the case of the representative DAT array, the reduction was 1.1 and 3.1 per cent. Using total production instead of average annual production produces similar percentage sized reductions. Moreover, if we compare the percentage reduction in both production measures for the high soiling scenario relative to the medium soiling scenario, the percentage reductions are in the order of 2.4, 2.2 and 2.0 per cent, respectively, for the representative FT, SAT and DAT arrays.

These results indicate that the output of the representative FT array is more adversely affected by increased soiling relative to the solar PV yields of the representative SAT and DAT arrays. This is seen in the higher percentage reduction rates associated with the FT array when compared with the other two representative arrays. Furthermore, the SAT array is more adversely affected by soiling than is the DAT array with the former recording higher percentage reductions in solar PV yield than the latter. Thus, some tracking ability can help partially insulate against the adverse impacts of module soiling on solar PV yield.

Recall that the key metric often sought when comparing the performance of solar PV tracking systems relative to a benchmark FT system is the extent to which output of the tracking systems exceeds that of the benchmark FT system. These results are reported in Panels (A)-(C) of Table 5 in relation to the annual production data reported in Table 4 for the low, medium and high soiling scenarios, respectively. The data in Table 5 documents the percentage increase in output of the SAT and DAT trackers relative to the output of the FT array. As such, in Table 5, Panel (A) for year 2007, the values of 24.6% and 38.8% indicate that the output of the SAT and DAT arrays recorded in Table 4, Panel (A) for year 2007 (e.g. 1491.4 and 1661.7 MWh's) are 24.6 and 38.8 per cent higher than the corresponding output of the FT array (e.g. 1197.1 MWh). Note that for the SAT technology, the percentages reported in the second column of Table 5 are calculated for each year as:

$$Percentage_{SAT} = \left[\frac{\left(\Pr od_{SAT} - \Pr od_{FT}\right)}{\Pr od_{FT}} \right] \times 100. \tag{3}$$

where $'\Pr od_{FT}'$ and $'\Pr od_{SAT}'$ refer to the yearly annual production data reported in Table 4 for the FT and SAT arrays. The percentages for the DAT technology listed in Column 3 of

Table 5 can also be calculated in a similar manner after replacing the 'SAT' subscripts in (3) with 'DAT' subscripts.

Examination of Table 5 once again indicates some year-on-year variation in the percentage figures and also by soiling scenario. For the SAT array, they are bounded between 20.5 and 25.9 per cent for the low soiling scenario [Panel (A)], between 20.8 and 26.1 per cent for medium soiling scenario [Panel (B)], and between 21.0 and 26.4 per cent for the high soiling scenario [Panel (C)]. The average percentage increase in solar PV yield for this array type relative to the solar PV yield of the benchmark representative FT array for the period 2007-2015 are listed in the last row of each panel in Table 5 and are 23.9, 24.1 and 24.3 per cent, respectively, for the low, medium and high soiling scenarios. Thus, the average results listed in Table 5 for the representative SAT array generally increases with the soiling scenario indicating that the SAT array tracking behaviour improves the solar PV yield relative to the benchmark FT array as the level of soiling increases, at least, for the monthly soiling ranges outlined in Table 2.

In the case of the representative DAT array, the results in Table 5 are bounded between 33.6 and 39.5 per cent for the low soiling scenario [Panel (A)], between 34.1 and 40.0 per cent for medium soiling scenario [Panel (B)], and between 34.9 and 40.6 per cent for the high soiling scenario [Panel (C)]. The average percentage increase in solar PV yield for this array relative to production from the benchmark FT array for the period 2007-2015 are 38.0, 38.4 and 39.1 per cent, respectively, for the low, medium and high soiling scenarios. Once again, the increase in the average value with soiling scenario indicates that the DAT array's tracking behaviour improves the solar PV yield relative to the FT array as the level of soiling increases. Furthermore, relative to the output of the benchmark FT array, the higher percentage values for the DAT array in Table 5 also clearly underpin the greater production of electricity coming from the DAT array compared with the SAT array.

Table5. Percentage Change in Production for SAT and DAT Tracking Systems Relative to FT System by Soiling Scenario

Panel (A): Low soiling rates

Year	SAT	DAT
2007	24.6	38.8
2008	24.7	38.7

2009	24.4	39.4
2010	22.4	36.3
2011	23.1	37.7
2012	24.6	38.6
2013	25.9	39.2
2014	24.8	39.5
2015	20.5	33.6
Average	23.9	38.0

Panel (B): Medium soiling rates

Year	SAT	DAT
2007	24.8	39.3
2008	24.9	39.2
2009	24.6	39.8
2010	22.5	36.7
2011	23.3	38.2
2012	24.8	38.8
2013	26.1	39.7
2014	25.0	40.0
2015	20.8	34.1
Average	24.1	38.4

Panel (C): High soiling rates

Year	SAT	DAT
2007	25.0	39.9
2008	25.2	39.9
2009	24.9	40.5
2010	22.6	37.3
2011	23.5	38.7
2012	25.0	39.2
2013	26.4	40.5
2014	25.3	40.6
2015	21.0	34.9
Average	24.3	39.1

The average results cited in the last row of each panel of Table 5 are broadly consistent with findings in the literature. Manufacturer's claims often assert increases of up to 30% for single axis tracking systems and up to 40% for dual axis tracking systems (Sabry and Raichle, 2013). Robinson and Raichle (2012) cite values from studies for SAT systems of between 29.3% and 42% and between 29.2% and 54%, depending upon the geographic location and climatic conditions underpinning the studies. Mousazadeh et al. (2009, p. 1802) cite general evidence pointing to gains of between 30% and 40% in good areas (and conditions) and in the low 20% range in poor conditions such as cloudy and hazy locations. More generally, in their detailed survey of efficiency gains reported in the literature relating to active solar tracking systems, they report evidence pointing to gains in production in the range of 20% to 30% for single axis tracking systems and between 30% and 45% for two axis tracking systems (Mousazadeh et al., 2009, pp. 1807-1810). Using these results as a broad guide, the average results reported in Table 5 would seem to be within the mid-range of these estimates cited in the broader literature.

(3.3) Assessment of Simulated Annual Capacity Factor Outcomes

Once the annual production outcomes have been calculated for the three representative arrays at GSRF, it is a simple process to calculate the annual capacity factor (ACF) outcomes of each representative system. The ACF is calculated by the following equation:

$$ACF = \left[\frac{Annual\_\Pr od}{\left(8760 \times System\_Capacity\right)} \right], \tag{4}$$

where '8760' represents the number of hours in a year assuming a 365 day year. Note, in this context, that for the leap years 2008 and 2012, the additional day corresponding to the 29th of February was dropped from the analysis. Note also in the denominator of (4), the kW system capacity concept we use in calculating the ACF is the sent-out capacity linked to the kWac maximum capacity of each of the inverters. This can be contrast with the use of the Array kWdc maximum capacity which is used to calculate the ACF results reported in the summary table generated by the SAM software. The ACF results for the three representative arrays are reported in Table 6, Panels (A) –(C) for the low, medium and high soiling scenarios. Note that the production concept [e.g. variable $'Annual\_\Pr od'$ in (4)] is based on the annual production totals for each soiling scenario cited in Table 4 and variable $'System\_Capacity'$ corresponds to the 630 kWac capacity limit of the inverter.

Table6. Energy Sent-out ACF by Representative Array Type by Soiling Scenario[1]

Panel (A): ACF: Low soiling rates

Year	FT	SAT	DAT
2007	21.7	27.0	30.1
2008	21.7	27.0	30.1
2009	22.3	27.8	31.1
2010	19.2	23.5	26.2
2011	20.6	25.4	28.4
2012	21.7	27.0	30.0
2013	22.3	28.1	31.0
2014	22.7	28.3	31.7
2015	21.7	26.1	29.0
Average	21.5	26.7	29.7

Panel (B): ACF: Medium soiling rates

Year	FT	SAT	DAT
2007	21.4	26.7	29.8
2008	21.4	26.7	29.7
2009	22.0	27.4	30.7
2010	19.0	23.2	25.9
2011	20.3	25.1	28.1
2012	21.4	26.7	29.7
2013	22.0	27.7	30.7
2014	22.4	28.0	31.3
2015	21.4	25.8	28.7

[1] Because of satellite problems, data was missing from the BOM's hourly solar irradiance dataset for: (1) year 2008, 14 to 17 of March and 10-13 of April, representing 192 hours of missing data; and (2) year 2009, 17-18 of February, 12 and 16-27 of November, representing 360 hours of missing data. The ACF calculations in Table 6 for years 2008 and 2009 were adjusted appropriately to account for these missing observations, with the number of hours in the denominator of equation (4) being reduced from 8760 to 8568 (e.g. 8760-192) and 8400 (e.g. 8760-360) for years 2008 and 2009, respectively.

Average	21.2	26.4	29.4

Panel (C): ACF: High soiling rates

Year	FT	SAT	DAT
2007	20.9	26.1	29.2
2008	20.8	26.1	29.2
2009	21.4	26.7	30.1
2010	18.5	22.7	25.4
2011	19.8	24.5	27.5
2012	20.9	26.1	29.0
2013	21.4	27.1	30.1
2014	21.8	27.3	30.7
2015	20.9	25.3	28.1
Average	20.7	25.8	28.8

Inspection of Table 6 points to considerable variation in the ACF's on a year-by-year basis, as was also observed with the production totals listed in Table 4. Specifically, and mirroring the production outcomes, the lowest ACF's were recorded in year 2010 and the highest were recorded in 2014. For the low, medium and high soiling scenarios, the ACF results for the benchmark FT technology fall within the range 19.2% to 22.7%, 19.0% to 22.4% and 18.5% to 21.8%. For the period 2007 to 2015, the average ACF values for the representative FT array were determined to be 21.5, 21.2 and 20.7 per cent for the low, medium and high soiling scenarios.

In the case of the representative SAT array, the equivalent ACF outcomes for each soiling scenario were in the range of 23.5% to 28.3%, 23.2% to 28.0% and 22.7% to 27.3%, respectively, and with average ACF outcomes being 26.7, 26.4 and 25.8 per cent. For the representative DAT array, the equivalent ACF outcomes were in the range of 26.2% to 31.7%, 25.9% to 31.3% and 25.4% to 30.7%, respectively. The average ACF outcomes by soiling scenario for the representative DAT array were 29.7, 29.4 and 28.8 per cent.

It is apparent from these results that for all three representative arrays, the average ACF results and their range clearly diminish as the level of module soiling increases. Moreover, mirroring the production results examined in the previous section, the ACF outcomes are highest for the representative DAT array, being in the range of 28.8 to 29.7 per cent, in average terms, depending on module soiling. This is followed by the results for the representative SAT array which, in average terms, are in the range 25.8 to 26.7 per cent, once again depending on soiling effects. Finally, the representative FT array clearly has the lowest results with average ACF results for the period 2007-2015 in the range of 20.7 to 21.5 per cent, depending on the extent of module soiling.

(4) Conclusions

Economic assessment of the viability of different types of solar PV tracking technologies centres on an assessment of whether the annual production of the different tracking technologies is increased enough relative to the benchmark FT system to compensate for the higher cost of installation and operational expenditures incurred by the tracking systems. To assess this, in the first instance, simulation modelling of the PV yield of the different solar PV systems needs to be performed. In this paper we restricted attention to an assessment of the production results of three representative 630 kW FT, SAT and DAT arrays located at UQ Gatton campus.

NREL's SAM model was used to simulate electricity production from the three representative solar PV systems installed at Gatton. Data relating to hourly solar irradiance data, weather data, and surface albedo data for Gatton was sourced from the BOM and NASA. Technical data relating to both module and inverter characteristics were sourced from both the module and inverter manufacturer's data sheets. Impacts of soiling and near-object shading were also accounted for in assessing solar PV yield.

Three broad module soiling scenarios were incorporated into the modelling. These were a low, medium and high module soiling scenario. These soiling scenarios were linked to a hypothesised cleansing effect of rainfall and were also augmented to account for energy gains and losses associated with divergence of local spectrum conditions from STC spectrum conditions. These low, medium and high augmented soiling losses produced average annualised soiling rates of 1.7, 3.2 and 5.7 per cent, respectively, albeit with much more variability arising on a month-by-month basis.

A key finding from the SAM simulations was that over the period 2007 to 2015, average increases in annual production of between 23.9 and 24.3 per cent and 38.0 and 39.1 per cent were obtained for the SAT and DAT tracking systems relative to the FT system, depending on module soiling rates. These results fell within the mid-range of estimates for these types of solar PV technologies identified in the broader literature.

ACF results were also calculated for the three representative arrays being considered. The representative FT array had the lowest recorded ACF values, in the range 20.7 to 21.5 per cent, depending on the rate of module soiling. The representative SAT array had the next lowest average ACF values, in the range 25.8 to 26.7 per cent, once again, depending upon module soiling rates. The highest ACF outcomes were recorded by the representative DAT array with average ACF results in the range of 28.8 to 29.7 per cent.

A key finding was that the output of the representative FT array is more adversely affected by increased soiling relative to the solar PV yields of the representative SAT and DAT arrays. Moreover, the SAT array was more adversely affected by soiling than was the DAT array. This suggested that some tracking ability could help partially insulate solar PV yields against the adverse impacts of module soiling. Future research will compare these predictions to actual data from the GSRF array.

References

ACT: Australian Capital Territory (2016) ‘: ACT Government, Environment and Planning Directorate, Environment, Large Scale Solar.’ Available at: http://www.environment.act.gov.au/energy/cleaner-energy/large-scale-solar.

AGL (2015) ‘Fact Sheet: Nyngan Solar Plant.’ Available at: https://www.agl.com.au/~/media/AGL/About%20AGL/Documents/How%20We%20Source%20Energy/Solar%20Community/Nyngan%20Solar%20Plant/Factsheets/2014/Nyngan%20Fact%20Sheet%20v7.pdf.

ARENA (2016) ‘Australian Government Australian Renewable Energy Agency.’ Available at: http://arena.gov.au/..

ARUP (2015) ‘Energy Yield Simulations, Module Performance Comparison for Four Solar PV Module Technologies.’ Arup (Pty) Ltd Consulting Engineers, Johannesburg, South Africa, May 2015. Available at: http://www.bizcommunity.com/f/1505/Module_Performance_Comparison_for_Four_Solar_PV_Module_Technologies_08-0....pdf.

Australian Government Clean Energy Regulator: CER (2016) ‘Large-scale Renewable Energy Target.’ Available at: http://www.cleanenergyregulator.gov.au/RET/About-the-Renewable-Energy-Target/How-the-scheme-works/Large-scale-Renewable-Energy-Target. Accessed 25-5-2016.

Bureau of Meteorology: BOM (2015) ‘Australian Hourly Solar Irradiance Gridded Data.’ Available at: http://www.bom.gov.au/climate/how/newproducts/IDCJAD0111.shtml.

CEFC (2016) ‘Clean Energy Finance Corporation.’ Available at: http://www.cleanenergyfinancecorp.com.au/.

Dobos, A (2012) ‘An improved Coefficient Calculator for the California Energy Commission 6 Parameter Photovoltaic Module Model’. *Journal of Solar Energy Engineering*, **132(2)**.

First Solar (2015) ‘Module Characterisation: Energy Prediction Adjustment for Local Spectrum’. First Solar Document Number PD 5-423.

Gilman, P. (2015) ‘SAM Photovoltaic Model Technical Reference.’ National Renewable Energy laboratory (NREL), May. Available at: http://www.nrel.gov/docs/fy15osti/64102.pdf.

Green Energy Markets (2015) ‘Renewables target needs 3,800MW of large scale renewables within 12 months.’ Available at: http://greenmarkets.com.au/news-events/renewables-target-needs-3800mw-of-large-scale-renewables-within-12-months.

Kimber, A., Mitchell, L., Nogradi, S., and H. Wenger (2006),’ The effect of soiling on large grid-connected photovoltaic systems in California and the southwest region of the United States.’ *In Conference Record of the 2006 IEEE 4th World Conference on Photovoltaic*

Energy Conversion, Waikoloa, HI, 2006. Available at: http://ieeexplore.ieee.org/stamp/stamp.jsp?tp=&arnumber=4060159.

Mousazadeh, H., Keyhani, A., Javadi, A., and H. Mobli (2009) 'A review of principle and sun-tracking methods for maximising solar systems output', *Renewable and Sustainable Energy Reviews*, 13, pp. 1800-1818.

NASA (2015) 'Albedo 16-Day L3 Global 0.05Deg CMG'. Available at: https://lpdaac.usgs.gov/dataset_discovery/modis/modis_products_table/mcd43c3.

RMI: Rocky Mountain Institute and Georgia Tech Research Institute (2014) 'Lessons From Australia: Reducing Solar PV Costs Through Installation Labour Efficiency.' Available at: http://www.rmi.org/Knowledge-Center/Library/2014-11_RMI-AustraliaSIMPLEBoSFinal.

Reda, I., and A. Andreas (2003) 'Solar position algorithm for solar radiation applications', National Renewable Energy Laboratory (NREL), Technical Report NREL/TP-560-34302. Available at: http://www.nrel.gov/docs/fy08osti/34302.pdf.

Robinson, J.W., and B.W. Raichle (2012) 'Performance Comparison of Fixed, 1-, and 2-Axis Tracking Systems for Small Photovoltaic Systems with Measured Direct Beam Fraction.' Proceedings of 42nd ASES Annual Conference, Denver, Colorado, May 2012. Available at: http://ases.conference-services.net/resources/252/2859/pdf/SOLAR2012_0261_full%20paper.pdf.

Sabry, M. S., and B. W. Raichle (2013) 'Determining the Accuracy of Solar Trackers'. *Proceedings of 42nd ASES Annual Conference*, Baltimore, Maryland, April 2013. Available at: http://proceedings.ases.org/wp-content/uploads/2014/02/SOLAR2013_0075_final-paper.pdf.

Sallaberry, F., de Jalon, A.G., Torres, J-L., and R. Pujol-Nadal (2015) 'Optical losses due to tracking error estimation for a low concentrating solar collector.' *Energy Conservation and Management*, **92**, pp. 194-206.

Stafford, B., Davis, M., Chambers, J., Martinez, M., and D. Sanchez (2009) 'Tracker accuracy: field experience, analysis, and correlation with meteorological conditions.' Photovoltaic Specials Conference (PVSC), 34 IEEE, June 2009. Available at: http://ieeexplore.ieee.org/stamp/stamp.jsp?tp=&arnumber=5411362.

Tapia Hinojosa., M (2014) 'Evaluation of Performance Models against Actual Performance of Grid Connected PV Systems.'Master's Thesis, Institute of Physics, Carl von Ossietzky Universität Oldenburg. Available at: http://oops.uni-oldenburg.de/2433/7/Thesis_TapiaM.pdf.

Thevenard, D., Driesse, A., Turcotte, D., and Y. Poissant (2010) 'Uncertainty in Long-term Photovoltaic Yield Projections.' CanmetENERGY, Natural Resources Canada, March. Available at: https://www.nrcan.gc.ca/sites/www.nrcan.gc.ca/files/canmetenergy/files/pubs/2010-122.pdf.

UQ (2015a) 'UQ, First Solar to build world-leading research centre.' Available at: https://www.uq.edu.au/news/article/2013/10/uq-first-solar-build-world-leading-research-centre

UQ (2015b) 'Fixed Tilt Array.' Available at: https://www.uq.edu.au/solarenergy/pv-array/content/fixed-tilt-array.

UQ (2015c) 'Single Axis tracking Array.' Available at: https://www.uq.edu.au/solarenergy/pv-array/content/single-axis-tracking-array.

UQ (2015d) 'Dual Axis tracking Array.' Available at: https://www.uq.edu.au/solarenergy/pv-array/content/dual-axis-array.

Appendix A. SAM Design and Parameter Settings

Panel (A): Modules

Description	Value	Measurement Unit
Module description - Thin Film Cadmium Telluride module	First Solar FS-395 PLUS (95 W)	NA
Cell type – CdTe	NA	NA
Module area	0.72	m^2
Nominal operating cell temperature	45	°C
Maximum power point voltage (Vmp)	45.8	V
Maximum power point current (Imp)	2.08	A
Open circuit voltage (Voc)	58	V
Short circuit current (Isc)	2.29	A
Temperature coefficient of Voc	-0.28	%/ °C
Temperature coefficient of Isc	0.04	%/ °C
Temperature coefficient of maximum power point	-0.29	%/ °C
Number of cells in series	146	NA
Standoff height	Ground or rack mounted	NA
Approximate installation height	one story building height or lower	NA

Panel (B): Inverters

Description	Value	Measurement Unit
Inverter type	SMA Sunny Central 720CP XT	NA
Maximum AC power output	630,000	Wac
Manufacturer efficiency	98.6	%
Maximum DC input power	638,945	Wdc
Nominal AC voltage	324	Vac
Maximum DC voltage	1000	Vdc
Maximum DC current	1400	Adc
Minimum MPPT DC voltage	577	Vdc
Nominal DC voltage	577	Vdc
Maximum MPPT DC voltage	850	Vdc
Power consumption during operation	1950	Wdc
Power consumption at night	100	Wac

Panel (C): System Design

Description	Value	Measurement Unit
Modules per string	15	NA

Strings in parallel	480	NA
Number of inverters	1	NA
Configuration at reference conditions		
Modules:		
Nameplate capacity	685.901	kWdc
Number of modules	7,200	NA
Total module area	5,184	m^2
Total land area	4.3	acres
Inverters:		
Nameplate capacity – on output	630.000	kWac
Nameplate capacity – on input	638.945	kWdc

Panel (D): Losses

Description	FT Value (%)	SAT Value (%)	DAT Value (%)
DC Array Losses			
Mismatch	1.1	1.1	1.1
Diodes and connections	0.0	0.0	0.0
DC wiring	1.5	1.5	1.5
DC tracking losses	0.0	0.45	0.42
Nameplate DC power loss	1.0	1.0	1.0
DC power optimisation	0.0	0.0	0.0
Total DC losses	3.56	3.99	3.96
AC System losses			
AC wiring	1.0	1.0	1.0
Transformer losses	1.15	1.15	1.15
Total AC Losses	2.14	2.14	2.14
Constant sky diffuse shading factor	4.45	1.96	1.1